

**Review**

## Aspects of Deep Ocean Mixing

CHRIS GARRETT\* and LOUIS ST. LAURENT

*School of Earth and Ocean Sciences, University of Victoria, Victoria, British Columbia, Canada*

(Received 18 June 2001; in revised form 14 September 2001; accepted 18 September 2001)

**The turbulent motions responsible for ocean mixing occur on scales much smaller than those resolved in numerical simulations of oceanic flows. Great progress has been made in understanding the sources of energy for mixing, the mechanisms, and the rates. On the other hand, we still do not have adequate answers to first order questions such as the extent to which the thermohaline circulation of the ocean, and hence the earth's climate, is sensitive to the present mixing rates in the ocean interior. Internal waves, generated by either wind or flow over topography, appear to be the principle cause of mixing. Mean and eddy flows over topography generate internal lee waves, while tidal flows over topography generate internal tides. The relative importance of these different internal wave sources is unknown. There are also great uncertainties about the spatial and temporal variation of mixing. Calculations of internal tide generation are becoming increasingly robust, but we do not know enough about the subsequent behavior of internal tides and their eventual breakdown into turbulence. It does seem, however, that most internal tide energy flux is radiated away from generation sites as low modes that propagate over basin scales. The mechanisms of wave-wave interaction and topographic scattering both act to transfer wave energy from low modes to smaller dissipative scales.**

Keywords:

- Ocean mixing,
- internal tides,
- internal waves,
- turbulence.

### 1. Introduction

A fundamental problem faced by oceanographers throughout the history of our field has been the difficulty of adequate sampling. Until recently, data collection has been limited in both time and space. The consequence was a tendency to assume that the ocean is rather steady in its behavior and that patterns of temperature, salinity, and currents are rather large scale. To be sure, this assumption was in clear conflict with the easily observed small scales of variability, and rapid temporal development, of oceanographic features such as the Kuroshio. Oceanographers clung for many years to a hope that the open ocean would be different, with large-scale unchanging features that could easily be depicted in ocean atlases.

This simple view had to be abandoned in the 1970s following the scientific discovery of eddy features in the ocean with time scales of the order of a month, space scales of the order of 100 km, and current speeds many times greater than the mean flow (e.g., Robinson, 1983).

Measurements in many other parts of the open ocean, reinforced more recently by data from satellite altimetry (e.g., Wunsch and Stammer, 1998), have led to the realization that the current at any one place is highly variable, and that the spatial scale of the currents is small compared with the scale of ocean basins. Nonetheless, oceanographers continued to hope that large-scale patterns of flow, averaged over many eddies, are rather unchanging in time. Even this hope is now being replaced with recognition that the frequency spectrum of oceanic motions is rather red, such that the definition of a mean current itself is problematic in many regions of the ocean (Wunsch, 1996).

Along with these studies of the large-scale and slow behavior of the ocean, there has been increasing recognition that ocean circulation may be sensitive to the rates of mixing associated with small-scale, high-frequency, processes such as breaking internal waves. These will be described more later, but the point to be made in this introduction is that, when discussing the mixing rate, lack of data and a hope that the ocean is simple led us to think of a single universal number for the vertical mixing rate. This view perhaps came easily from classic papers such

---

\* Corresponding author. E-mail: garrett@uvphys.phys.uvic.ca

as that of Munk (1966), with his inference of a diapycnal diffusivity  $K_v$  of about  $10^{-4} \text{ m}^2\text{s}^{-1}$  in the ocean interior.

If pressed, a physical oceanographer would have admitted that there was no reason to suppose that this mixing rate should be universal and constant. It is only very recently, however, that we are beginning to appreciate just how spatially variable the mixing rate is. We may not yet have an adequate appreciation of how much it also varies in time.

Evaluating the spatial and temporal variability of oceanic mixing requires an understanding of the mixing mechanisms and of the processes responsible. This is one theme of the present, rather selective, review. We shall describe the background and importance of ocean mixing in Section 2, then in Section 3 briefly discuss internal waves which seem to be the main cause of mixing. The internal tide is discussed in more detail in Section 4. The paper concludes in Section 5 with a discussion of what we regard as key scientific questions.

## 2. The Importance of Mixing

The simplest view of the thermohaline circulation of the oceans involves dense water sinking at high latitudes and then spreading equatorward and upwelling. As discussed by Munk and Wunsch (1998), for example, one might expect the abyssal ocean to fill completely with cold dense water all the way up to the surface where the water could be warmed and made lighter again by solar heating. Vertical mixing prevents the realization of such oceanic structure. This simultaneously leads to a diffuse thermocline, an increased meridional overturning rate, and an increased meridional heat flux. The power law dependences of these variables on the vertical diffusivity,  $K_v$ , depend on the assumptions made about the surface boundary condition (Bryan, 1987; Huang and Chou, 1994), but the existence of the dependence seems to clearly demonstrate the global significance of the mixing rate and its important role in affecting the earth's climate.

In reality, the density surfaces in the ocean are not flat, partly as a consequence of the contribution of wind forcing to ocean circulation. Surface isopycnals away from sinking regions at high latitudes penetrate to a depth of about 1 km at low latitudes. It thus seemed that water properties down to about this depth might be directly determined by the surface forcing at outcrops and diapycnal movement in the surface mixed layer, rather than by diapycnal mixing and diapycnal flow in the stratified thermocline. Fitting observed profiles below this depth, however, to a model assuming a balance between upwelling and downward diffusion required a basin-average vertical diffusivity of about  $10^{-4} \text{ m}^2\text{s}^{-1}$  (Munk, 1966; Munk and Wunsch, 1998). This implies a local rate of creation of potential energy at a rate  $K_v \rho N^2$ , with  $\rho$  the density and  $N$  the local buoyancy frequency. With the

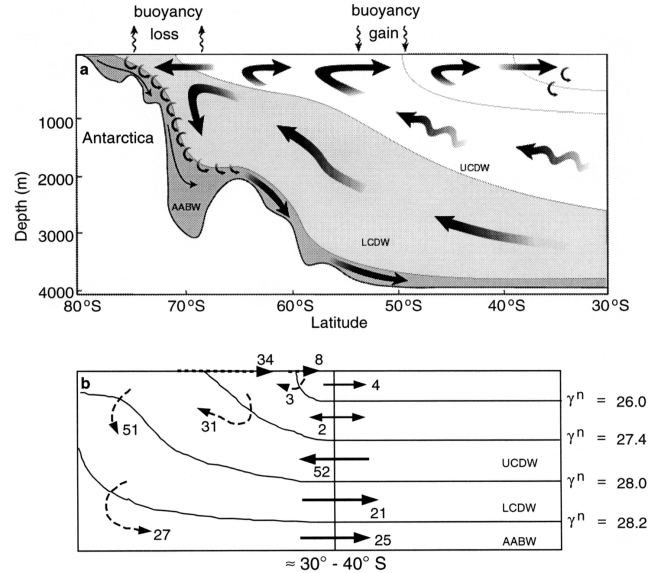


Fig. 1. Panel a: Schematic showing the physical aspects of the meridional overturning circulation in the Southern Ocean. Ekman pumping, air-sea buoyancy fluxes, and diapycnal exchanges all influence the circulation. (Adapted from Speer *et al.* (2000), courtesy of K. Speer.) Panel b: Schematic showing estimates of net transport (units =  $10^6 \text{ m}^3\text{s}^{-1}$ ) along (solid arrows) and across (dashed arrows) neutral density ( $\gamma^n$ ) layers in the latitude range between 30°–40°S. (Adapted from Sloyan and Rintoul (2001), courtesy of B. Sloyan.) The density layers corresponding to Upper Circumpolar Deep Water (UCDW), Lower Circumpolar Deep Water (LCDW), and Antarctic Bottom Water (AABW) are labeled in each panel.

assumption that the total mechanical energy input had to be at least 5 times this, Munk and Wunsch (1998) estimated a global requirement of about 2 TW, with perhaps half coming from internal tides and half coming from the wind. Both of these requirements appeared plausible.

This view is now being challenged (e.g., Toggweiler and Samuels, 1998; Gnanadesikan, 1999). In particular, Webb and Suginohara (2001) argue that Antarctic Bottom Water only has to be modified by diapycnal mixing until its density is the same as that of Circumpolar Deep Water. At this point it is upwelled to the sea surface by Ekman suction and modified further by air-sea fluxes, rather than by diapycnal mixing in the interior. A somewhat similar picture has been presented by Speer *et al.* (2000) and Sloyan and Rintoul (2001), though they argue for more interior mixing (Fig. 1). Importantly, the scenario of Webb and Suginohara (2001) reduces the energy requirements for mixing considerably, perhaps to only 0.6 TW rather than the 2 TW of Munk and Wunsch (1998). There is clearly considerable uncertainty. The resolution of these issues will determine the sensitivity of the earth's

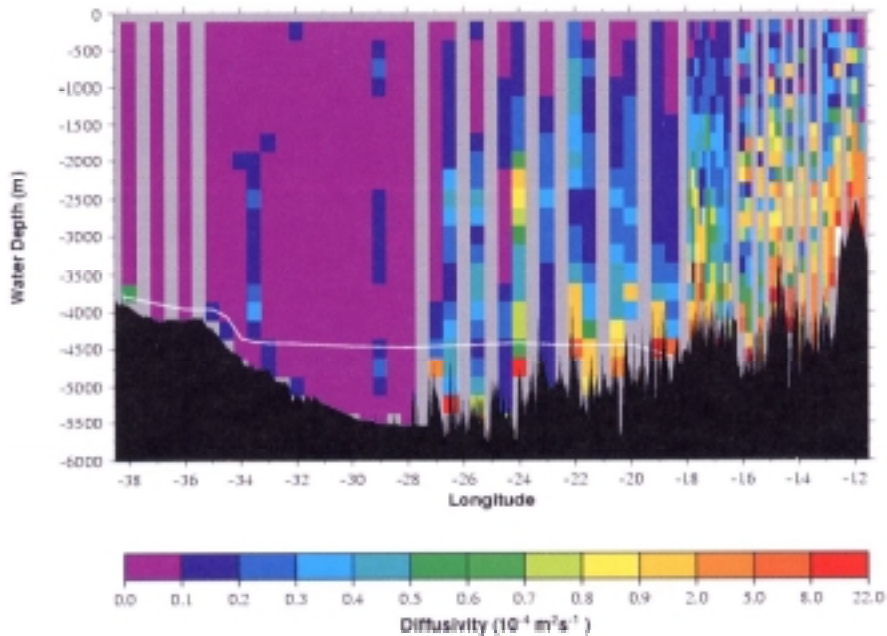


Fig. 2. A section of turbulent diffusivity across the Brazil Basin. The diffusivity estimates were made using observations of velocity microstructure which were averaged into 200 m vertical bins. The depth-longitude section was assembled from transects spanning a range of latitudes, and sampled during 1996 and 1997. Bottom bathymetry from one representative transect is shown; the apex of the Mid Atlantic Ridge along this transect is at 12°W. The white line shows the depth of the 0.8°C isotherm. (From Toole *et al.* (1997), courtesy of J. Toole.)

climate to vertical mixing in the ocean: the mixing rate in the stratified ocean interior may be a key factor, or so unimportant that taking it to be zero except in some abyssal regions would not be badly wrong.

At true abyssal depths there is, in fact, very clear evidence from some deep basins of the necessity of mixing: cold, dense, water that enters a basin at a measured rate and leaves at a higher temperature (and lower density) must have acquired heat by downward diffusion (e.g., Hogg *et al.*, 1982). Some of this mixing is associated with strong turbulence in the flow through the constrictive passages themselves (e.g., Ferron *et al.*, 1998), but this only affects the densest water, and some mixing for lighter waters must occur within the basins. A recently documented example is the Brazil Basin, where the spatially averaged diapycnal diffusivity at several density levels has to be several times  $10^{-4} \text{ m}^2 \text{ s}^{-1}$  (Morris *et al.*, 2001). It has long been recognized that this mixing need not be spatially uniform but could be concentrated near boundaries (Munk, 1966; Armi, 1978; and see the review by Garrett *et al.*, 1993). This suggestion is supported by a remarkable section of the observed energy dissipation rate across the Brazil Basin (Fig. 2), showing enhanced dissipation, and hence mixing, over the rough topography of the Mid Atlantic Ridge (Polzin *et al.*, 1997; Toole *et al.*, 1997).

This study strongly suggests the involvement of bottom topography in oceanic mixing, at least at abyssal depths. A modulation of the dissipation rate over the spring-neap tidal cycle also points to the involvement of internal tides as a key ingredient (Ledwell *et al.*, 2000). It cannot be ruled out, however, that there is some subtle interaction between the tides and the topography that also involves wind-generated internal waves. It remains a scientific challenge to account quantitatively for the total dissipation in the water column, to explain its vertical profile, and to determine the relative importance of wind- and tidally generated internal waves in causing the mixing.

### 3. Internal Waves in the Ocean

Internal oscillations in the stratified ocean are associated with internal waves in the frequency band from the local Coriolis frequency  $f$  to the buoyancy frequency  $N$ . Significant progress has been achieved over the last few decades in describing the way in which energy is typically distributed in a parameter space that may be defined by the wave frequency  $\omega$  and the vertical wavenumber  $m$ . A picture has also emerged which envisages nonlinear interactions between existing waves as causing a cascade to higher vertical wavenumbers, with an associated increase of vertical shear. This cascade eventually leads to

shear instability on a vertical scale that is typically on the order of a meter (but varying by at least an order of magnitude in either direction, depending primarily on the energy level of the waves).

The theories behind this scenario were based on weak interaction theory (McComas and Müller, 1981a) or on a separation of scales between large-scale and small-scale waves (Henyey *et al.*, 1986). As reviewed by Müller *et al.* (1986), neither of these approaches is really valid, but we have been tempted to accept the results because the two different approaches gave rather similar answers and because semi-empirical syntheses by Gregg (1989) and Polzin *et al.* (1995) seemed to agree with mixing levels implied by turbulence measurements. The theory and data both converged on a diapycnal mixing rate in the main thermocline of no more than 1 or 2 times  $10^{-5} \text{ m}^2\text{s}^{-1}$  for typical internal wave energy levels. This level of mixing was also observed in a direct tracer release experiment (Ledwell *et al.*, 1998). The small mixing rate is consistent with a slow leakage of energy from the internal waves. Hence, only moderate changes in overall wave energy levels occur over time scales longer than the time between generation events, consistent with the generally observed persistence of internal waves and lack of an “internal calm.” The weak mixing also suggests that diapycnal mixing in the main thermocline of the ocean is of minor importance.

We referred earlier to the situation in abyssal basins, where much higher mixing rates are both expected and observed. These seem to be associated with elevated internal wave energy levels. Remarkably high diapycnal mixing rates, inferred from high levels of internal wave shear measured by a Lowered ADCP, have also been found throughout the water column in the Southern Ocean by Polzin and Firing (1997). They suggested that the observed waves were generated as lee waves by strong mean and eddy flow over the rough bottom topography, rather than by tidal currents or surface wind. Direct inference of a vertical mixing rate from internal wave energy levels is still risky, however. As stressed by Sun and Kunze (1999a, b), the assumptions underlying the basic theoretical models are difficult to justify, and these models have been validated for only the most commonly observed internal wave spectra. For example, Kunze *et al.* (2001) find that the parameterizations in terms of finescale variables underestimate mixing in parts of Monterey Submarine Canyon by a factor of 30.

Nagasawa *et al.* (2000) suggest that sampling of internal wave activity and turbulence has missed key locations and times of strong mixing. They argue that energetic near-inertial waves generated by fall and winter storms at midlatitudes in the North Pacific Ocean propagate equatorward until their (conserved) frequency is equal to twice the local inertial frequency. At this point

strong “Parametric Subharmonic Instability” (PSI) can occur, transferring energy to waves with half the frequency and much smaller vertical scales, thus setting the stage for shear instability and mixing. This is a provocative and important suggestion. The predicted seasonal changes in mixing rates are much larger than the factor of two observed between winter and summer during the North Atlantic Tracer Release Experiment (Ledwell *et al.*, 1998), but the limited latitude range of the tracer observations may account for this discrepancy.

It must also be admitted that there is considerable uncertainty about nonlinear internal wave interaction rates in general. Some twenty years after major accomplishments in theoretical studies of these interactions, as reviewed by Müller *et al.* (1986), it is perhaps time for these theories to be revisited. In particular, the behavior of the energetic near-inertial waves is not well described. The wave-wave interaction theories have tended to take the inertial wave part of the spectrum as a prescribed background field which affects other waves; the rate of transfer of energy out of the inertial band seems to be uncertain. Further attention to nonlinear interactions including both inertial waves and internal tides is also needed, given the prominence of both these frequencies. Mihaly *et al.* (1998) find a significant peak in current spectra at a frequency given by the sum of inertial and tidal frequencies, suggesting an important interaction. This interaction can, however, be a purely advective process in which fine-scale vertical structure in the inertial currents is advected vertically by the internal tide (Alford, 2001a). More investigation is required of the potentially key interaction between near-inertial waves and the internal tide.

Just as importantly, one must recognize that the wave-wave interactions are not occurring in an infinite medium of uniform properties. As stressed by Hirst (1991) and D’Asaro (1991), the most energetic components of the internal wave spectrum are those large-scale (low mode) waves which have a travel time over the depth of the ocean rather shorter than the time scale for nonlinear interactions in the ocean interior. Thus, interactions with the rough topography of the seafloor may also be important for shaping the internal wave spectrum. In particular, topographic scattering (Müller and Xu, 1992) and reflection off sloping boundaries (Garrett and Gilbert, 1988; Eriksen, 1998), transfer energy from large to small wavelengths, thereby increasing the probability of shear instability and mixing. On the other hand, interactions with the seafloor, unlike nonlinear interactions in the ocean interior, will not generally move energy in the frequency domain.

We thus do not really know where internal waves are dissipating and causing mixing. It may be throughout the ocean interior as a consequence of nonlinear interactions there, or it may be mainly in the abyssal ocean after

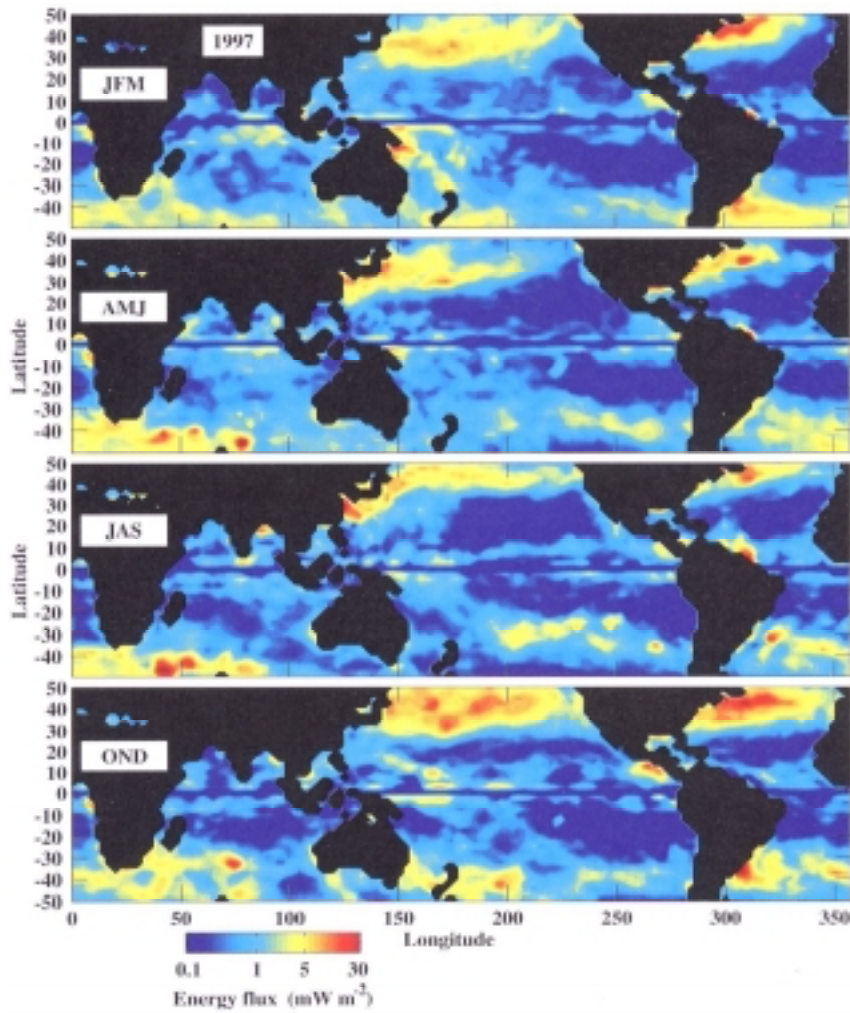


Fig. 3. Seasonally averaged maps of energy flux into near-inertial mixed layer motions for the year 1997, based on a model using observed climatological values of the mixed layer depth. (From Alford (2001b), courtesy of M. Alford.)

topographic interactions. It is quite likely that all of these processes are important.

A gross constraint on the amount of mixing that can be caused by internal waves can come from consideration of the amount of energy going into the waves. Alford (2001b) has estimated that the total amount of energy going into near-inertial internal waves as a consequence of their generation by wind. He finds that the energy input into the upper ocean is very variable spatially (Fig. 3), but about  $1 \text{ mW m}^{-2}$  on average, or approximately 0.3 TW globally. In a similar study, Hibiya and Watanabe (2001) estimate a global energy flux of 0.7 TW. Both of these estimates are less than the 1 TW claimed by Munk and Wunsch (1998), though Wunsch (1998) estimated that about 1 TW goes into geostrophic currents, and it is quite possible that some of this finds its way into internal lee waves generated by steady and eddy currents flowing over rough bottom topography. Polzin and Firing (1997) con-

sider this to be an important source of internal waves in the Southern Ocean. In general, though, the strongest currents near the seafloor are those associated with the tides. We turn next to a more detailed discussion of internal wave generation by tidal flow over rough topography.

#### 4. Internal Tide Driven Mixing in the Deep Ocean

##### 4.1 Energetics of internal tide mixing

While mean flows and eddy activity in the deep ocean are generally characterized by  $O(1) \text{ mm s}^{-1}$  currents, barotropic tidal currents in the deep ocean are  $O(10) \text{ mm s}^{-1}$ . Tides may be the dominant source of mechanical energy for stirring and mixing through internal waves. Munk and Wunsch (1998) review the evidence that tidal forces do about 3.7 TW of work on the global ocean, with 2.5 TW contributed by the semidiurnal lunar tides alone.

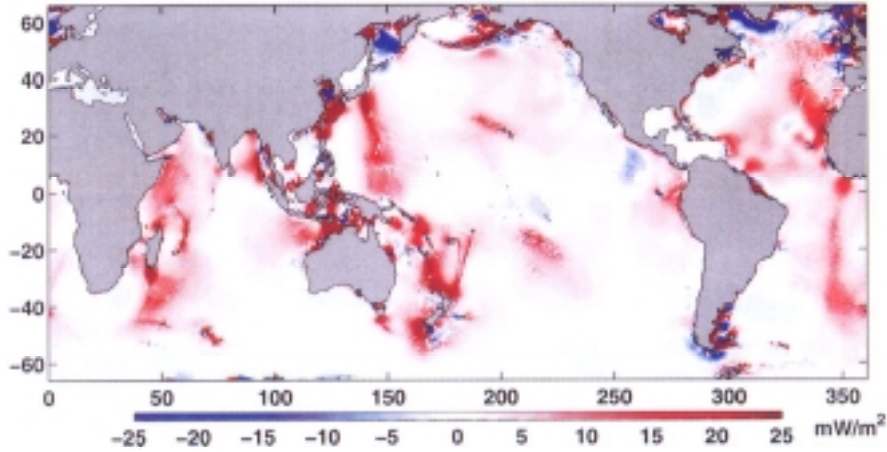


Fig. 4. Global distribution of barotropic tidal loss. The estimates were made using observations of sea surface elevation from the Topex/Poseidon altimeter. Negative values indicate regions where noise prevented accurate estimates. (From Egbert and Ray (2001), courtesy of G. Egbert.)

Egbert and Ray (2000, 2001) have examined least-square fits of Topex/Poseidon altimetry data to models for the global barotropic tide, and they interpret model residuals in terms of “tidal dissipation,” with this referring to any mechanisms that transfer energy out of the barotropic tides. They are not able to distinguish whether barotropic energy is lost to baroclinic waves (the internal tide) or to bottom friction. About 0.7 TW of power is lost from  $M_2$  barotropic tides in the deep ocean (Fig. 4). The part of this associated with frictional dissipation can be estimated by the relation  $\rho c_d |u| u^2$ , where  $c_d = 0.0025$  is the drag coefficient. For typical open ocean tidal speeds  $u \approx 0.03 \text{ m s}^{-1}$ , and the frictional dissipation is less than  $0.1 \text{ mW m}^{-2}$ , or less than 30 GW globally. Thus, nearly all barotropic power conversion in the deep ocean must occur as internal tide generation. The remaining tidal power loss occurs through frictional dissipation in shallow seas.

Egbert and Ray (2000, 2001) and Niwa and Hibiya (2001) identify a number of deep ocean regions where barotropic tidal energy is likely being transferred to internal tides. These regions are generally associated with three types of topography: (i) oceanic island chains, (ii) oceanic trenches, and (iii) mid-ocean ridges. Oceanic islands, such as those on the Hawaiian Ridge and the Izu Ridge, and oceanic trenches such as those in the west Pacific Ocean, are steep topographic features with typical slopes  $s$  (rise over run) of 0.1 to 0.3 (Seibold and Berger, 1996). Niwa and Hibiya (2001) comment on the much greater internal tide energy levels in the western and central Pacific than in the eastern Pacific. Egbert and Ray (2000, 2001) identify the oceanic islands of Micronesia and Melanesia as sites accounting for over 100 GW of internal tide production while Hawaii accounts for 20 GW. Mid-ocean ridges have smaller slopes than oceanic

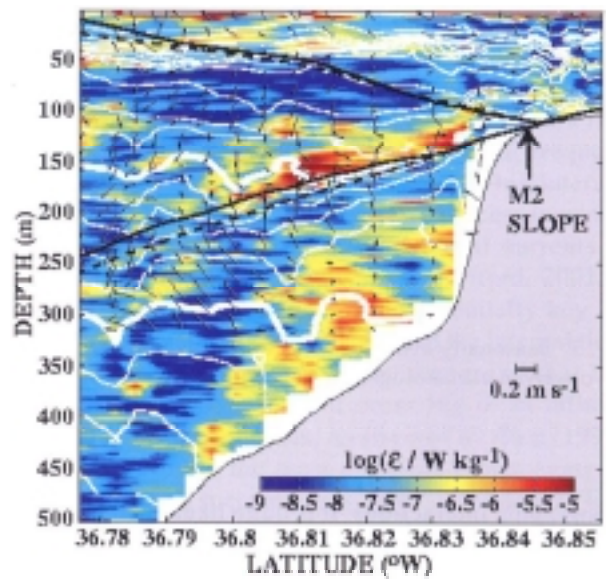


Fig. 5. A section of turbulent dissipation rate  $\epsilon$  off the shelf break slope in Monterey Bay, California. Black arrows show horizontal currents, and white lines show density surfaces. The ray paths of semidiurnal internal tide beams emanating from the shelf break are shown (solid black lines). The dashed black lines show the ray paths including the effect of vertical shear. (From Lien and Gregg (2001), courtesy of R.-C. Lien and M. Gregg.)

island chains or trenches, but Egbert and Ray (2000, 2001) identify mid-ocean ridge topography in the Atlantic and Indian Oceans as each accounting for over 100 GW of internal tide production.

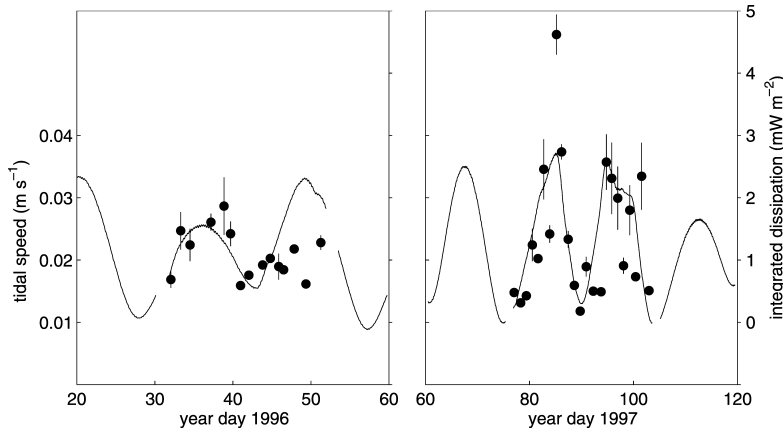


Fig. 6. Vertically integrated turbulent dissipation rates from the Brazil Basin. The dissipation rate observations were integrated to 2000 m above the bottom, and daily averages of multiple integrated profiles are shown with standard deviations. A record of daily averaged barotropic tidal speed along the transect track is also shown. (From St. Laurent *et al.*, 2001.)

#### 4.2 Observations of internal tides and mixing

The contribution of internal tides to oceanic velocity and temperature records has long been recognized. Wunsch (1975) and Hendershott (1981) present reviews of earlier work. Renewed interest in internal tides came with observations of sea surface elevation from the Topex/Poseidon altimeter. These observations have been used to constrain hydrodynamic models of the tides, and hence produce accurate estimates of open-ocean barotropic tides (Egbert *et al.*, 1994; Egbert, 1997). A multi-year record of observations is now available, and the semidiurnal tides  $M_2$  and  $S_2$  can be extracted from the record. Ray and Mitchum (1996) used along-track Topex/Poseidon records to examine the surface manifestation of internal tides generated along the Hawaiian Islands. They found that both first and second baroclinic modes of the semidiurnal internal tides were present in the data, and that the signal of internal-tide propagation can be tracked up to 1000 km away from the Hawaiian Ridge. In a further analysis of the altimetry data, Ray and Mitchum (1997) estimate that 15 GW of semidiurnal internal tide energy radiates away from the Hawaiian Ridge in the first baroclinic mode. Topex/Poseidon altimetry records have also been used by Cummins *et al.* (2001) to show that internal tides generated at the Aleutian Ridge can be tracked over 1000 km into the central Pacific. There, the total internal tide energy flux is only about 2 GW.

Microstructure observations have provided direct observations of internal tide driven mixing at steep topography (Lueck and Mudge, 1997; Kunze and Toole, 1997; Lien and Gregg, 2001). Lueck and Mudge (1997) attributed enhanced turbulence at Cobb Seamount in the northeast Pacific to a semidiurnal internal tide, finding the largest turbulence levels along a beam of internal tide energy emanating from the seamount rim. Kunze and

Toole (1997) describe microstructure observations from Fieberling Seamount in the northeast Pacific, with the largest mixing levels at the summit of the seamount where diurnal internal tide energy was trapped. Internal tides are also produced along the continental margins of the ocean basins, and evidence of internal tide driven mixing at Monterey Canyon off California was reported by Lien and Gregg (2001). They produced an elegant section of dissipation data extending off the slope of the continental shelf (Fig. 5), showing enhanced turbulence levels along the ray path of a semidiurnal internal tide beam out to more than 4 km away from the topography. Maximum diffusivities along the internal tide beam were about  $10^{-2} \text{ m}^2\text{s}^{-1}$ , as had also been found by Kunze and Toole (1997) and Lueck and Mudge (1997) at Fieberling and Cobb Seamounts respectively.

Evidence of internal tide driven mixing in the abyssal ocean was obtained as part of the Brazil Basin Tracer Release Experiment (Ledwell *et al.*, 2000), conducted near the Mid Atlantic Ridge. St. Laurent *et al.* (2001) find maximum levels of vertically integrated dissipation of  $3 \text{ mW m}^{-2}$ , modulated over the spring-neap tidal cycle with a small lag of about a day (Fig. 6). These observations span a network of fracture zones west of the Mid Atlantic Ridge, with topographic relief varying by up to 1 km between the crests and floors of abyssal canyons. The dominant topography of the fracture zone system has a slope less than 0.1, as the canyons are generally 30 to 50 km wide. Elevated turbulent dissipation rates were found along all regions of the fracture zone topography, but turbulence levels appeared most enhanced over the slopes. Above all classes of topography, turbulence levels decrease to background levels, consistent with  $K_v \approx 10^{-5} \text{ m}^2\text{s}^{-1}$ , more than 1000 m above the bottom.

### 4.3 Theory

There are many questions regarding the internal tide's role in deep ocean mixing. What is the energy flux into internal tides? How is this energy converted to turbulence? How efficient are wave-wave interactions at converting energy at large scales into energy at small, dissipative scales? Are internal tides likely to dissipate near their generation site, or far away? Here, we discuss some of these issues using existing theory.

Internal tides are produced in stratified regions where barotropic tidal currents flow over topography. Internal tides radiate throughout the oceans with frequencies identical to those of the barotropic tides ( $M_2$ ,  $S_2$ ,  $K_1$ ,  $O_1$ , etc.) and their harmonics, provided that the frequency  $\omega$  falls in the range  $f < \omega < N$ . Poleward of the inertial latitudes, where  $\omega = f$ , internal tides are trapped over topography (e.g., Nakamura *et al.*, 2000). Thus, while internal tides of diurnal frequency can only propagate freely equatorward of about  $\pm 30^\circ$  latitude, semidiurnal tides are freely propagating within  $\pm 74.5^\circ$  latitude.

For a given wavenumber component  $k$  of topography with amplitude  $a$ , four nondimensional parameters characterize the internal waves generated by the tidal flow. Two parameters,  $\omega/f$  and  $\omega/N$ , specify the time scale of the tide relative to the inertial and buoyancy time scales. The two additional parameters are dynamically more significant. One of these parameters,  $ku_0/\omega$ , measures the ratio of the tidal excursion amplitude  $u_0/\omega$  to the horizontal scale of the bathymetry  $k^{-1}$ . This parameter also measures the ratio of the barotropic tidal speed  $u_0$  to the wave speed  $\omega/k$ . The remaining parameter,  $ka/\alpha$ , measures the ratio of topographic slope  $s = ka$  to the slope  $\alpha$  of a radiated tidal beam, where

$$\alpha = \frac{k}{m} = \left( \frac{\omega^2 - f^2}{N^2 - \omega^2} \right)^{1/2}. \quad (1)$$

The tidal excursion parameter serves to classify two regimes of interest. In one regime, the tidal excursion is less than the scale of the bathymetry. The waves of this "internal tide" regime radiate mainly at the fundamental frequency of the tide. In the other regime, the tidal excursion exceeds the length scale of the bathymetry. This is referred to as the "quasi-steady lee wave" regime, with waves that propagate only in the instantaneous up-stream direction with frequencies  $-kU(t)$  and phase speeds  $-U(t)$  relative to the current. Quasi-steady lee waves manifest themselves mainly as higher harmonic internal tides.

The steepness parameter,  $s/\alpha$ , is also used to distinguish two regimes. Topography is referred to as "supercritical" when its slope is greater than the slope of a tidal beam so that  $s/\alpha > 1$ , while "subcritical" topography has a slope less steep than a tidal beam so that  $s/\alpha <$

1. Using Eq. (1) with  $\omega = 1.4 \times 10^{-4} \text{ s}^{-1}$ ,  $N = 10^{-3} \text{ s}^{-1}$ , and  $f = 10^{-4} \text{ s}^{-1}$  gives  $\alpha = 0.1$  and provides a reference value for the slope of an  $M_2$  tidal beam in the deep ocean. It follows that many oceanic island chains and trench features are supercritical, while large-scale features of mid-ocean ridge topography are subcritical.

The equations for internal tide generation at supercritical topography are reviewed by Baines (1982), and solutions for specific topographic geometries can be computed using ray tracing methods. Solutions for ridge, slope, and shelf topography have been discussed by Rattray (1960), Baines (1982), and Craig (1987). A simplified model for internal-tide generation at a topographic step was proposed by Stigebrandt (1980) and applied to deep ocean topographies by Sjöberg and Stigebrandt (1992). However, the equations for arbitrary supercritical topography  $h(\mathbf{x})$  are difficult to solve due to the necessity of a nonlinear bottom boundary condition,  $w(h) = \mathbf{U} \cdot \nabla h + \mathbf{u}(h) \cdot \nabla h$ , where  $\mathbf{U}$  is the barotropic current vector and  $(\mathbf{u}, w)$  are the lateral and vertical components of the baroclinic velocity. The baroclinic wave response to barotropic tidal flow over arbitrary steep topography has instead been studied using numerical simulations. In particular, numerical studies have been carried out for internal tides at the Hawaiian Ridge (Holloway and Merrifield, 1999; Merrifield *et al.*, 2001) and the Aleutian Ridge (Cummins *et al.*, 2001). The properties of quasi-steady lee waves have also been studied numerically for atmospheric (Lott and Teitelbaum, 1993) and oceanographic (Nakamura *et al.*, 2000) cases.

Models for internal-tide generation by subcritical topography have been developed by Cox and Sandstrom (1962), Baines (1973), Bell (1975a, b), Hibiya (1986), and Llewellyn Smith and Young (2001). These models apply a linearized bottom boundary condition  $w(-H) = \mathbf{U} \cdot \nabla h$ . Two approximations are made in this linearization: (i) the neglect of the term  $\mathbf{u}(h) \cdot \nabla h$  involving the lateral current vector  $\mathbf{u}$  of the internal tide, and (ii) the use of a constant depth  $z = -H$  in place of  $z = h(\mathbf{x})$  in applying the boundary condition. Both of these approximations are justified when  $s/\alpha \ll 1$ . With application of the linear boundary condition, solutions for arbitrary bathymetry can be obtained by superposition.

Bell (1975a, b) considered internal waves generated at subcritical topography in an ocean of infinite depth. His theory is applicable in both the internal tide and quasi-steady lee wave regimes. The vertical energy flux  $E_f$  is a quantity of primary interest and is often expressed as  $E_f = \langle pw \rangle$  using the wave pressure  $p$ , or as the product  $E_f = c_g E$  between the vertical group speed  $c_g$  and the wave energy density  $E$ . Bell's (1975b) expression for the energy flux produced from bathymetry with a (one-sided) power spectrum  $\phi(k)$  is

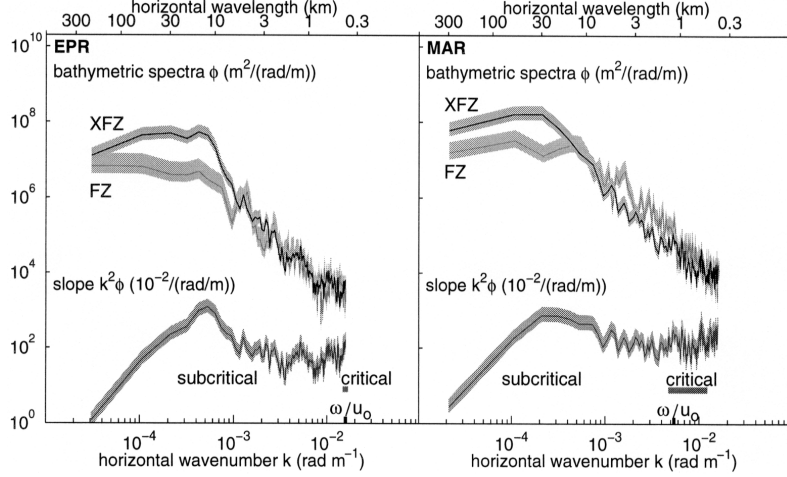


Fig. 7. Bathymetric spectra for the East Pacific Rise (EPR) and the Mid Atlantic Ridge (MAR) from sections taken along fracture zones (FZ) and across fracture zones (XFZ). The standard deviations of the spectral estimates are represented by the shaded bands. In each panel, the slope spectra of the XFZ bathymetry are also shown. The wavenumber for the tidal excursion scale  $\omega/u_0$  is shown for each site. The ranges of wavenumbers associated with subcritical and critical slopes are also indicated. (From St. Laurent and Garrett, 2001.)

$$E_f = 2\rho_0 \sum_{n=1}^{n_N} n\omega \left( (N_b^2 - n^2\omega^2)(n^2\omega^2 - f^2) \right)^{1/2} \int_0^\infty k^{-1} J_n^2(ku_0/\omega) \phi(k) dk, \quad (2)$$

where  $N_b$  is the buoyancy frequency at the bottom and  $J_n$  is the Bessel function. The index  $n$  corresponds to tidal harmonics, with the maximum harmonic  $n_N$  being the largest integer less than  $N_b/\omega$ . In Eq. (2), the power spectrum is normalized to satisfy  $\int_0^\infty \phi(k) dk = \overline{h^2}$ , where  $\overline{h^2}$  is the mean square height of the topography.

St. Laurent and Garrett (2001) have considered internal-tide generation at mid-ocean ridge topography using high resolution bathymetric data from the East Pacific Rise (EPR) and the Mid Atlantic Ridge (MAR). Spectra of bathymetry from these regions are shown in Fig. 7, with sections taken along fracture zones (FZ) and sections taken across fracture zones (XFZ). Slope spectra follow directly from the bathymetric spectra as  $k^2\phi(k)$ , and the slope spectra for the XFZ sections are also shown in Fig. 7. The mean square slope ( $\overline{s^2}$ ) out to any wavenumber  $k$  can be calculated by integrating the slope spectrum

$$\overline{s(k)^2} = \int^k k'^2 \phi(k') dk'. \quad (3)$$

In general, there will exist some wavenumber  $k_c$  where  $s(k_c) = \alpha$ ; the slope corresponding to critical generation

of a tidal beam. The topographic slopes on scales greater than  $k_c^{-1}$  are subcritical, while the topographic slopes on scales less than  $k_c^{-1}$  are supercritical. The possible range of critical slope wavenumbers for the EPR and MAR data is shown in Fig. 7b and corresponds to topography with horizontal wavelengths of roughly 1 km. The length scale corresponding to the amplitude of the tidal excursion  $u_0/\omega$  was also calculated for the  $M_2$  tides at these sites. Tidal excursion amplitudes in the XFZ sections are 53 m and 185 m for the EPR and MAR sites respectively, based on  $M_2$  tidal current amplitudes of  $u_0 = 0.008 \text{ m s}^{-1}$  (EPR) and  $u_0 = 0.026 \text{ m s}^{-1}$  (MAR) obtained from the tidal model of Egbert *et al.* (1994).

St. Laurent and Garrett (2001) also present calculations of internal-tide energy flux for these mid-ocean ridge sites. The integrated energy fluxes for the XFZ sections (Fig. 8) are roughly  $0.2 \text{ mW m}^{-2}$  and  $4.3 \text{ mW m}^{-2}$  for the EPR and MAR sites respectively. The larger energy flux at the MAR is attributable to rougher bathymetry and stronger tidal currents.

Baroclinic modes of internal tides have been discussed by Wunsch (1975), Hibiya (1986), Khatiwala (2001), and Llewellyn Smith and Young (2001). The modal dispersion relation is

$$k_j = \frac{j\pi}{H} \left( \frac{\omega^2 - f^2}{N^2 - \omega^2} \right)^{1/2}, \quad (4)$$

for  $j = 1, 2, \dots$ . Llewellyn Smith and Young (2001) also discuss the influence of depth varying stratification.

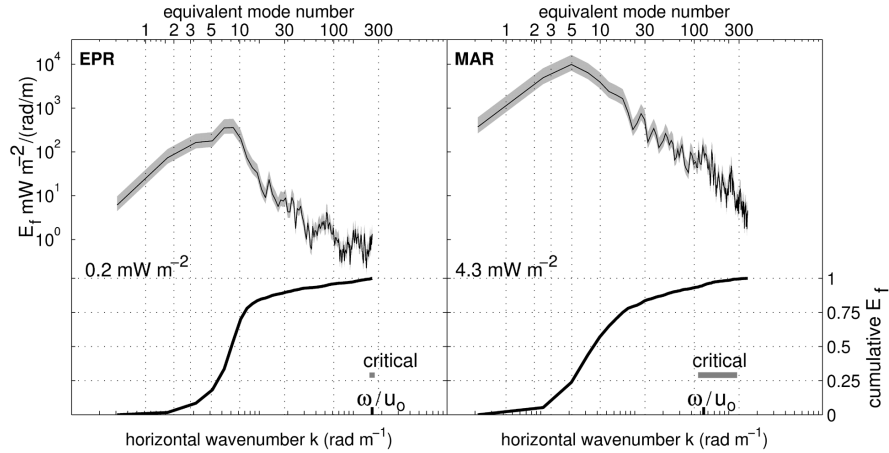


Fig. 8. Spectra and cumulative integrals of internal tide energy flux for the East Pacific Rise and Mid Atlantic Ridge sites. Equivalent modes estimated by Eq. (4) are given along the upper axis for reference. (From St. Laurent and Garrett, 2001.)

St. Laurent and Garrett (2001) suggest a finite depth correction to Bell’s theory by starting the integral in Eq. (2) at  $k = (1/2)k_1$  rather than  $k = 0$ . Figure 8 shows the cumulative integrated power along the full spectrum of wavenumbers for the XFZ sections. In both EPR and MAR cases, over 2/3 of the total power occurs in modes 1–10. Modes 1–30 contain over 80% of the total power.

Considerations for topography that varies in both lateral directions are discussed by Bell (1975b), Li (2001), Llewellyn Smith and Young (2001), and St. Laurent and Garrett (2001). Two wavenumbers of bathymetry ( $k, l$ ) must be considered, and the factor  $k^{-1}$  in Eq. (2) is replaced by  $(k^2 + l^2)^{-1/2}$ . Bell (1975b) and Li (2001) discuss a rectilinear tidal current. Llewellyn Smith and Young (2001) present the case of an arbitrary tidal current, but St. Laurent and Garrett (2001) show that the theory is simplified when the coordinate system is aligned with the major and minor axes of the tidal ellipse. Estimates for energy flux at MAR topography are comparable to the XFZ values described above.

Finite amplitude corrections to the subcritical approximation have been explored analytically (Balmforth *et al.*, 2001; St. Laurent and Garrett, 2001) and by numerical simulation (Khawiwala, 2001; Li, 2001). These studies suggest that subcritical estimates of energy flux are quite robust for finite slopes that are less than critical. Balmforth *et al.* (2001) find that critical sinusoidal topography produces 56% more energy flux than predicted by subcritical theory, though the increase for a Gaussian seamount is only 14%. The numerical results of Li (2001) indicate a 70% increase in energy flux for critical sinusoidal topography. For supercritical slopes, Li (2001) finds that mixing causes a reduction in the buoyancy stratification. This inhibits the generation of internal tides, with a significant decrease in energy flux, though this result is

sensitive to the model’s dissipation scheme. Khawiwala (2001) also finds reduced energy flux production at supercritical topography. Further research on supercritical generation is needed.

#### 4.4 Mechanisms of internal tide dissipation

Once generated, internal-tide energy will radiate off the bottom and will be stable to shear instability if the Richardson number  $Ri = N^2/u_z^2$  is greater than unity at all depths. The mean square shear ( $u_z^2$ ) of the radiated internal tide (in isolation from other currents with shear) can be computed for the case of subcritical topography by integrating a function of the bathymetric spectrum. St. Laurent and Garrett (2001) find that the estimated Richardson number of internal tides over fracture zone topography exceeds unity at all vertical wavelengths larger than O(10) m (equivalently, horizontal wavelengths larger than O(100) m). Thus, only a very small fraction of the internal-tide energy flux is likely to dissipate by shear instability immediately after generation from subcritical topography. Observations by Lueck and Mudge (1997) and Lien and Gregg (2001) suggest that high levels of shear and turbulence occur at sites of internal tide generation by supercritical topography, but the net dissipation at these sites may represent only a small fraction of the radiated internal tide energy.

The transfer of energy between wave modes due to wave-wave interactions has been the subject of a number of studies (e.g., McComas and Müller, 1981a, b; Henyey *et al.*, 1986; Hirst, 1991). Olbers and Pomphrey (1981) specifically examined the wave-wave interactions between the internal tide and the internal wave continuum, and estimated the time scale for energy transfer away from modes 1–10 to higher modes by Parametric Subharmonic Instability (PSI). This transfers tidal energy with fre-

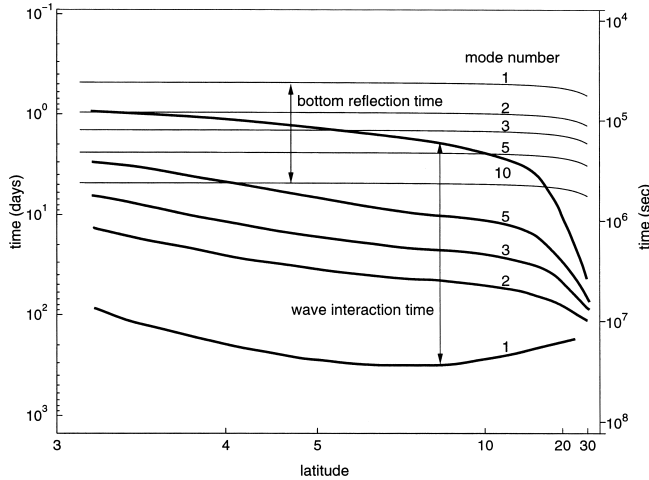


Fig. 9. The time scales for wave-wave interactions between the  $M_2$  internal tide and the internal wave continuum for modes 1, 2, 3, 5, and 10, adapted from Olbers (1983). The Parametric Subharmonic Instability interaction for the  $M_2$  tide occurs equatorward of  $30^\circ$  latitude. Bottom reflection times for the various modes were estimated for an exponential stratification over a depth of 4000 m. (From St. Laurent and Garrett, 2001.)

quency  $\omega$  to larger vertical wavenumbers with frequency  $\omega/2$ , and is thus an effective mechanism for dissipating the  $M_2$  internal tides at latitudes less than  $30^\circ$ . Estimates of the dissipation time scale for the  $M_2$  internal tides by PSI are given in Fig. 9 (adapted from Olbers, 1983). The transfer rate is  $O(100)$  days for mode 1, consistent with the observed slow southward decay of low mode internal tides generated at the Hawaiian Ridge (Ray and Mitchum, 1996) and the Aleutian Ridge (Cummins *et al.*, 2001). The PSI transfer time reduces to  $O(1)$  day for mode 10.

As stressed by Hirst (1991) and others, it is useful to compare the wave interaction time scale to the time for a wave group to travel from the bottom to the surface and back again. The travel time is defined as  $\tau = 2 \int_0^d c_g^{-1} dz$ , where the integral is over the ocean depth and  $c_g$  is the vertical component of the group velocity. The latitude and mode number dependent curves for  $\tau$  were computed using  $N = N_0 e^{z/b}$  with  $(b, N_0) = (1300 \text{ m}, 0.00524 \text{ s}^{-1})$ , and are shown in Fig. 9. Low modes have the fastest group speeds, with  $\tau \leq 12$  hrs for mode 1 and  $\tau \geq 4$  days for mode 10. Thus, internal-tide modes 1–5 will easily complete one round trip between the bottom and surface before experiencing the effects of wave-wave interactions. For modes greater than 10, energy transfer to higher modes will occur over a time scale comparable to, or less than, the bottom reflection time. Thus, wave-wave interactions may be the dominant mechanism of spectral evolution for high-mode components of the internal tide,

while bottom reflection is more significant for low modes.

It should also be mentioned that beams of internal tide energy that are stable in the ocean interior can induce a large response at the base of the surface mixed layer, possibly contributing to localized mixing there. Observations of this have been reported by New and Da Silva (2001), with theoretical treatments by Thorpe (1998) and Gerkema (2001).

## 5. Discussion

The study of mixing in the ocean interior is at an exciting, if complex, stage, with many questions awaiting resolution. This should be possible in the next few years. Some points to be borne in mind in designing future research programs are:

1) While mixing is clearly of first order importance in many abyssal basins, we really do not know how high in the water column this importance persists. It is possible that the general structure and circulation of the oceans, with the associated influence on climate, are insensitive to the rather small mixing rates in the main thermocline.

2) It may well be that the behavior of the surface layer is the most important oceanic component for the climate system. This behavior depends on mixing processes at the base of the surface layer. Internal waves generated by the wind, and possibly also by the tide, drive mixing at the base of the surface layer, but this has not been discussed in this brief review.

3) Inverse studies using existing oceanic data can help to determine the presence of diapycnal fluxes, but it is often difficult to know whether these are associated with mixing in the ocean interior or with air-sea transfer. As discussed by Tandon and Zahariev (2001) and in papers they cite, the diurnal cycle of mixing and restratification can make an important, though usually neglected, contribution to water mass transformation. Including this effect may remove the need for diapycnal mixing in the ocean interior that is otherwise called for by inverse models.

4) Even if mixing in the ocean interior is not that important for major issues of climate, it may still be a controlling process for things like biological productivity (e.g., Gargett and Marra, 2001; Yamazaki *et al.*, 2001) and waste disposal.

5) It is not clear whether mixing in the oceans is driven primarily by winds or by internal tides. While the contribution of wind forcing to mixing may occur primarily through wind-generated internal waves, internal lee waves generated at seafloor topography by low frequency currents (driven by the wind and also by the thermohaline forcing of the ocean) may also be important in some locations. The relative importance of wind- and tidally driven mixing is not known, but is likely to vary spatially.

6) The vertical structure of mixing induced by internal wave breaking is not well described or well understood. It does seem to be linked to underlying topography and is probably associated with topographic scattering of internal waves. A small amount of energy is likely lost each time an internal wave beam encounters topography. This occurs through both direct instability of the bottom-scattered waves and by nonlinear interactions occurring in the high wavenumber part of the scattered wave spectrum.

7) If mixing occurs primarily near ocean boundaries, we do not fully understand how this influences the ocean interior (though see McDougall (1991) and Garrett *et al.* (1993) for some discussion). This topic will not be pursued here, except to mention that an interesting question concerns the extent to which partially mixed fluid is exchanged with stratified fluid from the ocean interior. It is often assumed that this is necessary. However, on a sloping boundary, restratification can also be driven by local buoyancy forces (e.g., Garrett *et al.*, 1993).

8) Even if we know the amount of energy being lost from the internal wave field, it may not be valid to assume that a fixed fraction of this goes into the vertical buoyancy flux. As discussed by Garrett (2001), the mixing efficiency may be significantly reduced in strongly mixing regions near ocean boundaries.

9) One ultimate goal is to provide suitable formulae for use in numerical models of ocean circulation, with the mixing rate parameterized in terms of resolved variables. This pragmatic requirement needs to be borne in mind while we study the details of processes, but may be especially difficult considering the heterogeneity of bottom topography. Also, as stressed in the introduction, the vertical mixing rate in the ocean may be significantly time dependent as well as spatially variable.

10) In this brief review we have discussed only the mixing associated with internal wave breaking, but we should not forget that there are vast regions of the oceans where double-diffusive processes can occur (e.g., Schmitt, 1994). It seems likely that in most such regions double diffusion is less important than internal wave breaking (e.g., St. Laurent and Schmitt, 1999), but there may be parts of the oceans where double diffusion dominates.

11) Underlying our whole approach to ocean mixing and its parameterization is the assumption that there is a spectral gap between those processes responsible for mixing and larger scale, or more slowly varying, resolved flows. This dubious assumption is discussed further by Davis (1994) and Garrett (2001). The latter author concludes that its evident lack of validity may not be a major concern, but the question needs further attention.

Overall, we stress the importance of recognizing that, while we know much about mixing in the ocean, and certainly a great deal more than a decade ago, we are still a

long way from a full understanding and adequate parameterization.

### Acknowledgements

We thank Hide Yamazaki for the invitation to write this review and for his helpful suggestions. We are also most grateful to Eric Kunze and an anonymous reviewer for their valuable comments, and to those who provided figures reproduced in this article. Our studies are supported by the Natural Sciences and Engineering Research Council of Canada and by the U.S. Office of Naval Research.

### References

- Alford, M. H. (2001a): Fine-structure contamination: observations and a model of a simple two-wave case. *J. Phys. Oceanogr.*, **31**, 2645–2649.
- Alford, M. H. (2001b): Internal swell generation: The spatial distribution of energy flux from the wind to mixed-layer near-inertial motions. *J. Phys. Oceanogr.*, **31**, 2359–2368.
- Armi, L. (1978): Some evidence for boundary mixing in the deep ocean. *J. Geophys. Res.*, **83**, 1971–1979.
- Baines, P. G. (1973): The generation of internal tides by flat-bump topography. *Deep-Sea Res.*, **20**, 179–205.
- Baines, P. G. (1982): On internal tide generation models. *Deep-Sea Res.*, **29**, 307–338.
- Balmforth, N. J., G. R. Ierley and W. R. Young (2001): Tidal conversion by nearly critical topography. *J. Phys. Oceanogr.* (submitted).
- Bell, T. H. (1975a): Lee waves in stratified flows with simple harmonic time dependence. *J. Fluid Mech.*, **67**, 705–722.
- Bell, T. H. (1975b): Topographically generated internal waves in the open ocean. *J. Geophys. Res.*, **80**, 320–327.
- Bryan, F. (1987): Parameter sensitivity of primitive equation ocean general circulation models. *J. Phys. Oceanogr.*, **17**, 970–985.
- Cox, C. S. and H. Sandstrom (1962): Coupling of surface and internal waves in water of variable depth. *Journal of the Oceanographic Society of Japan, 20th Anniversary Volume*, 499–513.
- Craig, P. D. (1987): Solutions for internal tide generation over coastal topography. *J. Mar. Res.*, **45**, 83–105.
- Cummins, P. F., J. Y. Cherniawski and M. G. G. Foreman (2001): North Pacific internal tides from the Aleutian Ridge: Altimeter observations and modelling. *J. Mar. Res.*, **59**, 167–191.
- D’Asaro, E. A. (1991): A strategy for investigating and modeling internal wave sources and sinks. p. 451–465. In *Dynamics of Oceanic Internal Gravity Waves, Proc. ‘Aha Huliko’ a Hawaiian Winter Workshop*, ed. by P. Muller and D. Henderson, SOEST.
- Davis, R. E. (1994): Diapycnal mixing in the ocean: Equations for large-scale budgets. *J. Phys. Oceanogr.*, **24**, 777–800.
- Egbert, G. D. (1997): Tidal data inversion: Interpolation and inference. *Prog. Oceanogr.*, **40**, 81–108.
- Egbert, G. D. and R. D. Ray (2000): Significant dissipation of tidal energy in the deep ocean inferred from satellite altimeter data. *Nature*, **405**, 775–778.

- Egbert, G. D. and R. D. Ray (2001): Estimates of  $M_2$  tidal energy dissipation from TOPEX/POSEIDON altimeter data. *J. Geophys. Res.* (in press).
- Egbert, G. D., A. F. Bennett and M. G. G. Foreman (1994): TOPEX/POSEIDON tides estimated using a global inverse model. *J. Geophys. Res.*, **99**, 24821–24852.
- Eriksen, C. C. (1998): Internal wave reflection and mixing at Fieberling Guyot. *J. Geophys. Res.*, **103**, 2977–2994.
- Ferron, B., H. Mercier, K. Speer, A. Gargett and K. Polzin (1998): Mixing in the Romanche Fracture Zone. *J. Phys. Oceanogr.*, **28**, 1929–1945.
- Gargett, A. and J. Marra (2001): Effects of upper ocean physical processes—Turbulence, advection, and air-sea interaction—on oceanic primary production. In *The Sea: Biological-Physical Interactions in the Ocean*, ed. by A. R. Robinson, J. J. McCarthy and B. J. Rothschild, John Wiley & Sons (in press).
- Garrett, C. (2001): Stirring and mixing: What are the rate-controlling processes? p. 1–8. In *Proceedings of the Twelfth 'Aha Huliko' a Hawaiian Winter Workshop*, ed. by P. Muller and D. Henderson, SOEST.
- Garrett, C. and D. Gilbert (1988): Estimates of vertical mixing by internal waves reflected off sloping topography. p. 405–424. In *Small-Scale Turbulence and Mixing in the Ocean*, ed. by J. C. J. Nihoul and B. M. Janard, Elsevier Scientific.
- Garrett, C., P. MacCready and P. Rhines (1993): Boundary mixing and arrested Ekman layers: Rotating stratified flow near a sloping boundary. *Ann. Rev. Fluid Mech.*, **25**, 291–323.
- Gerkema, T. (2001): Internal and interfacial tides: Beam scattering and local generation of solitary waves. *J. Mar. Res.*, **59**, 227–255.
- Gnanadesikan, A. (1999): A simple predictive model for the structure of the oceanic pycnocline. *Science*, **283**, 2077–2079.
- Gregg, M. C. (1989): Scaling turbulent dissipation in the thermocline. *J. Geophys. Res.*, **94**, 9686–9698.
- Hendershott, M. C. (1981): Long waves and ocean tides. p. 292–341. In *Evolution of Physical Oceanography*, ed. by B. A. Warren and C. Wunsch, The MIT Press.
- Heney, F. S., J. Wright and S. M. Flatte (1986): Energy and action flow through the internal wave field: an eikonal approach. *J. Geophys. Res.*, **91**, 8487–8495.
- Hibiya, T. (1986): Generation mechanism of internal waves by tidal flow over a sill. *J. Geophys. Res.*, **91**, 7697–7708.
- Hibiya, T. and M. Watanabe (2001): Global estimates of the wind-induced inertial energy. *Geophys. Res. Lett.* (submitted).
- Hirst, E. (1991): Internal wave-wave resonance theory: Fundamentals and limitations. p. 211–226. In *Dynamics of Oceanic Internal Gravity Waves, Proc. 'Aha Huliko' a Hawaiian Winter Workshop*, ed. by P. Muller and D. Henderson, SOEST.
- Hogg, N. G., P. Biscaye, E. Gardner and W. J. Schmitz (1982): On the transport of Antarctic Bottom Water in the Vema Channel. *J. Mar. Res.*, **40**, Suppl., 231–263.
- Holloway, P. E. and M. A. Merrifield (1999): Internal tide generation by seamounts, ridges and islands. *J. Geophys. Res.*, **104**, 25,937–25,951.
- Huang, R. X. and R. L. Chou (1994): Parameter sensitivity study of the saline circulation. *Clim. Dyn.*, **9**, 391–409.
- Khaliwala, S. (2001): Generation of internal tides in the ocean. *Deep-Sea Res.* (submitted).
- Kunze, E. and J. M. Toole (1997): Tidally driven vorticity, diurnal shear, and turbulence atop Fieberling Seamount. *J. Phys. Oceanogr.*, **27**, 2663–2693.
- Kunze, E., L. K. Rosenfeld, G. S. Carter and M. C. Gregg (2001): Internal waves in Monterey Submarine Canyon. *J. Phys. Oceanogr.* (submitted).
- Ledwell, J. R., A. J. Watson and C. S. Law (1998): Mixing of a tracer in the pycnocline. *J. Geophys. Res.*, **103**, 21,499–21,529.
- Ledwell, J. R., E. T. Montgomery, K. L. Polzin, L. C. St. Laurent, R. W. Schmitt and J. M. Toole (2000): Mixing over rough topography in the Brazil Basin. *Nature*, **403**, 179–182.
- Li, M. (2001): Energetics of internal tides radiated from deep-ocean topographic features. *J. Phys. Oceanogr.* (submitted).
- Lien, R.-C. and M. C. Gregg (2001): Observations of turbulence in a tidal beam and across a coastal ridge. *J. Geophys. Res.*, **106**, 4575–4592.
- Llewellyn Smith, S. G. and W. R. Young (2001): Conversion of the barotropic tide. *J. Phys. Oceanogr.* (submitted).
- Lott, F. and H. Teitelbaum (1993): Linear unsteady mountain waves. *Tellus*, **45**, 201–220.
- Lueck, R. G. and T. D. Mudge (1997): Topographically induced mixing around a shallow seamount. *Science*, **276**, 1831–1833.
- McComas, C. H. and P. Müller (1981a): The dynamic balance of internal waves. *J. Phys. Oceanogr.*, **11**, 970–986.
- McComas, C. H. and P. Müller (1981b): Time scales of resonant interactions among oceanic internal waves. *J. Geophys. Res.*, **83**, 1397–1412.
- McDougall, T. (1991): Parameterizing mixing in inverse models. p. 355–386. In *Dynamics of Oceanic Internal Gravity Waves, Proc. 'Aha Huliko' a Hawaiian Winter Workshop*, ed. by P. Muller and D. Henderson, SOEST.
- Merrifield, M. A., P. E. Holloway and T. M. Shaun Johnston (2001): The generation of internal tides at the Hawaiian Ridge. *Geophys. Res. Lett.*, **28**, 559–562.
- Mihaly, S. F., R. E. Thomson and A. B. Rabinovich (1998): Evidence for nonlinear interaction between internal waves of inertial and semidiurnal frequency. *Geophys. Res. Lett.*, **25**, 1205–1208.
- Morris, M. Y., M. M. Hall, L. C. St. Laurent and N. G. Hogg (2001): Abyssal mixing in the Brazil Basin. *J. Phys. Oceanogr.*, **31**, 3331–3348.
- Müller, P. and N. Xu (1992): Scattering of oceanic internal waves off random bottom topography. *J. Phys. Oceanogr.*, **22**, 474–488.
- Müller, P., G. Holloway, F. Heney and N. Pomphrey (1986): Nonlinear interactions among internal gravity waves. *Rev. Geophys.*, **24**, 493–536.
- Munk, W. H. (1966): Abyssal recipes. *Deep-Sea Res.*, **13**, 707–730.
- Munk, W. and C. Wunsch (1998): Abyssal recipes II: energetics of tidal and wind mixing. *Deep-Sea Res.*, **45**, 1977–2010.
- Nagasawa, M., Y. Niwa and T. Hibiya (2000): Spatial and temporal distribution of the wind-induced internal wave energy

- available for deep water mixing in the North Pacific. *J. Geophys. Res.*, **105**, 13933–13943.
- Nakamura, T., T. Awaji, T. Hatayama and K. Akitomo (2000): The generation of large amplitude unsteady lee waves by subinertial K1 tidal flow: A possible vertical mixing mechanism in the Kuril Straits. *J. Phys. Oceanogr.*, **30**, 1601–1621.
- New, A. L. and J. C. B. Da Silva (2001): Remote-sensing evidence for the local generation of internal soliton packets in the central Bay of Biscay. *Deep-Sea Res. I* (in press).
- Niwa, Y. and T. Hibiya (2001): Numerical study of the spatial distribution of the  $M_2$  internal tide in the Pacific ocean. *J. Geophys. Res.* (in press).
- Olbers, D. J. (1983): Models of the oceanic internal wave field. *Rev. Geophys.*, **21**, 1567–1606.
- Olbers, D. J. and N. Pomphrey (1981): Disqualifying two candidates for the energy balance of oceanic internal waves. *J. Phys. Oceanogr.*, **11**, 1423–1425.
- Polzin, K. and E. Firing (1997): Estimates of diapycnal mixing using LADCP and CTD data from I8S. *International WOCE Newsletter*, **29**, 39–42.
- Polzin, K. L., J. M. Toole and R. W. Schmitt (1995): Finescale parameterizations of turbulent dissipation. *J. Phys. Oceanogr.*, **25**, 306–328.
- Polzin, K. L., J. M. Toole, J. R. Ledwell and R. W. Schmitt (1997): Spatial variability of turbulent mixing in the abyssal ocean. *Science*, **276**, 93–96.
- Rattray, M., Jr. (1960): On the coastal generation of internal tides. *Tellus*, **22**, 54–62.
- Ray, R. and G. T. Mitchum (1996): Surface manifestation of internal tides generated near Hawaii. *Geophys. Res. Lett.*, **23**, 2101–2104.
- Ray, R. and G. T. Mitchum (1997): Surface manifestation of internal tides in the deep ocean: observations from altimetry and island gauges. *Prog. Oceanogr.*, **40**, 135–162.
- Robinson, A. R. (ed.) (1983): *Eddies in Marine Science*. Springer-Verlag, 609 pp.
- St. Laurent, L. C. and C. Garrett (2001): The role of internal tides in mixing the deep ocean. *J. Phys. Oceanogr.* (submitted).
- St. Laurent, L. and R. W. Schmitt (1999): The contribution of salt fingers to vertical mixing in the North Atlantic Tracer Release Experiment. *J. Phys. Oceanogr.*, **24**, 1404–1424.
- St. Laurent, L. C., J. M. Toole and R. W. Schmitt (2001): Buoyancy forcing by turbulence above rough topography in the abyssal Brazil Basin. *J. Phys. Oceanogr.*, **31**, 3476–3495.
- Schmitt, R. W. (1994): Double diffusion in oceanography. *Ann. Rev. Fluid Mech.*, **26**, 255–285.
- Seibold, E. and W. H. Berger (1996): *The Sea Floor—An Introduction to Marine Geology*. Springer-Verlag, 356 pp.
- Sjöberg, B. and A. Stigebrandt (1992): Computations of the geographical distribution of the energy flux to mixing processes via internal tides and the associated vertical circulation in the ocean. *Deep-Sea Res.*, **39**, 269–291.
- Sloyan, B. M. and S. R. Rintoul (2001): Circulation, renewal and modification of Antarctic mode and intermediate water. *J. Phys. Oceanogr.*, **31**, 1005–1030.
- Speer, K., S. R. Rintoul and B. Sloyan (2000): The diabatic Deacon Cell. *J. Phys. Oceanogr.*, **30**, 3212–3222.
- Stigebrandt, A. (1980): Some aspects of tidal interaction with fjord constriction. *Estuar. Coast. Mar. Sci.*, **11**, 151–166.
- Sun, H. and E. Kunze (1999a): Internal wave-wave interactions. Part I: The role of internal wave vertical divergence. *J. Phys. Oceanogr.*, **29**, 2886–2904.
- Sun, H. and E. Kunze (1999b): Internal wave-wave interactions. Part II: Spectral energy transfer and turbulence production. *J. Phys. Oceanogr.*, **29**, 2905–2919.
- Tandon, A. and K. Zahariev (2001): Quantifying the role of mixed layer entrainment for water mass transformation in the North Atlantic. *J. Phys. Oceanogr.*, **31**, 1120–1131.
- Thorpe, S. A. (1998): Nonlinear reflection of internal waves at a density discontinuity at the base of the mixed layer. *J. Phys. Oceanogr.*, **28**, 1853–1860.
- Toggweiler, J. R. and B. Samuels (1998): On the ocean's large scale circulation near the limit of no vertical mixing. *J. Phys. Oceanogr.*, **28**, 1832–1852.
- Toole, J. M., J. R. Ledwell, K. L. Polzin, R. W. Schmitt, E. T. Montgomery, L. St. Laurent and W. B. Owens (1997): The Brazil Basin Tracer Release Experiment. *International WOCE Newsletter*, **28**, 25–28.
- Webb, D. J. and N. Sugimotohara (2001): Vertical mixing in the ocean. *Nature*, **409**, 37.
- Wunsch, C. (1975): Internal tides in the ocean. *Rev. Geophys.*, **13**, 167–182.
- Wunsch, C. (1996): *The Ocean Circulation Inverse Problem*. Cambridge University Press, 442 pp.
- Wunsch, C. (1998): The work done by the wind on the ocean circulation. *J. Phys. Oceanogr.*, **28**, 2331–2339.
- Wunsch, C. and D. Stammer (1998): Satellite altimetry, the marine geoid and the oceanic general circulation. *Annu. Rev. Earth Planet. Sci.*, **26**, 219–253.
- Yamazaki, H., D. L. Mackas and K. L. Denman (2001): Coupling small scale physical processes with biology. In *The Sea: Biological-Physical Interactions in the Ocean*, ed. by A. R. Robinson, J. J. McCarthy and B. J. Rothschild, John Wiley & Sons (in press).